I&EC research
Industrial & Engineering Chemistry Research

Article

pubs.acs.org/IECR

Effect of Chemical and Physical Cross-Linking on Tensile Characteristics of Solution-Blown Soy Protein Nanofiber Mats

S. Sinha-Ray,[†] S. Khansari,[†] A. L. Yarin,*[,†] and B. Pourdeyhimi[‡]

[†]Department of Mechanical and Industrial Engineering, University of Illinois at Chicago, 842 W. Taylor St., Chicago, Illinois 60607-7022, United States

[‡]3427 The Nonwovens Institute, Box 8301, North Carolina State University, Raleigh, North Carolina 27695-8301, United States

Supporting Information

ABSTRACT: Solution-blown soy protein/nylon 6 nanofibers, 40/60 and 50/50 wt/wt %, were collected on a rotating aluminum drum in order to form a mat. The collected fiber mats were bonded both chemically (using aldehydes and ionic cross-linkers) and physically (by means of wet and thermal treatment) to increase the tensile strength to increase the range of application of such green nonwovens. Chemical cross-linkers bond different amino groups, primary amides, and sulfhydryl groups in protein structure. This is beneficial for the enhancement of tensile strength. Such mechanical properties of soy-protein-containing nanofiber mats as Young's modulus, yield stress, and maximum stress and strain at rupture were measured for different cross-linkers at different contents. Overall, higher contents of cross-linking agents in soy protein nanofiber mats resulted in nanofibers with higher strength which was accompanied by a less plastic behavior. Treatment with ionic cross-linkers resulted in nanofiber mats with higher Young's modulus of the mats. Covalent bonds formed by aldehyde groups had a smaller effect on the mat strength. As cross-linked nanofibers were exposed to heat, the bonds formed between amino groups in the fibers were broken and they became less aggregated. The overall increase of about 50% in tensile strength as a result of thermal bonding under compression was observed. In addition, wet conglutination of soy protein/nylon 6 nanofiber mats for 24 h under 6 kPa pressure led to partial physical cross-linking of nanofibers and, consequently, to a 65% increase in Young's modulus. Solution-blown soy protein/nylon 6 nanofiber mats were also subjected to aging in water for 1 h at 80 °C. An enhancement in the tensile strength of soy protein nanofiber mats was revealed after the exposure to water, as well as a slight plasticizing effect.

1. INTRODUCTION

Biodegradable polymers attract attention in relation to such applications as food packaging, construction materials, composite fillers, wood adhesives, particle boards, etc.[1−3] Efforts have also been taken to reinforce nanofibers with cellulose nanocrystals.[4] Such a shift in attention is mainly because of the impetus of pushing toward the "green"-technology-driven products to reduce carbon footprints as much as possible. Biopolymers such as wheat gluten, soy protein, gelatin, casein, and corn zein are of high importance due to their abundance in nature and biodegradability. Zein and gluten can form stronger films, whereas their production and purification costs are much higher than those of soy protein. Low cost and abundance of soy protein makes it a unique plant protein, attractive for many applications. Soy-based nanofibers[5,6] seems to be one the best possible options, as textile and nonwoven industry is one of the largest consumers of petroleum-based polymers, and the solution blowing method is by far the best possible alternative to meltblowing, since the latter is incapable of forming fibers from soy proteins. Formation of micro- and nanofibers using soybean as a raw material is considered to be highly attractive.[7,8] However, many products made of biodegradable polymers possess low strength and high hydrophilicity.

The basic building blocks of proteins are amino acids which are linked by different covalent and ionic bridges (e.g., amide, disulfide, etc.). Reactivity of proteins depends on the side chains of their free amino acids. The labile groups in the side chains are attacked by cross-linking agents, and the resulting dints serve as the active sites for efficient inter- and intramolecular cross-linking. The chemically reactive groups in amino acids include carboxylic, primary and secondary amine, cystine, lysine, arginine, guanidyl, and sulfhydryl groups.[9,10] These reactive groups participate in cross-linking triggered by chemical cross-linkers or thermal treatment.

Solubility of soy protein in a solvent is determined by the competition of protein−protein interactions with protein−solvent interactions, which is related to the isoelectric point of soy protein. Therefore, soy protein solubility can be effectively influenced by pH, ionic strength, temperature, and soy protein concentration.[11] The most widely used cross-linkers for soy proteins include aldehyde groups, with formaldehyde being the oldest and most common agent.[11−15] Formaldehyde cross-links protein polyamide chains by reacting with −NH, −OH, and −SH groups. This reaction produces methylene bridges between polymer molecules.[12,16] Glyoxal is a small molecule compared to most aldehyde compounds and mostly bonds amino acid side chains in one molecule.[17,18] On the basis of the same logic, cellulose networks were also cross-linked by glyoxalization.[19] Therefore, the cross-linking effect of glyoxalization is restricted to intermolecular structure. Also, the cross-

Received: September 2, 2012
Revised: October 21, 2012
Accepted: November 1, 2012
Published: November 1, 2012

dx.doi.org/10.1021/ie302359x | Ind. Eng. Chem. Res. 2012, 51, 15109−15121

linking effect of zinc ions is determined by the way they bond to protein chains.[20−22] In addition to these, sodium borohydride, known as a strong reducing agent, can also be used as a cross-linker.

Thermal calender bonding is widely used in the nonwoven industry,[23] and in a sense, thermal treatment under compression employed in the present work mimics it. Several works dealt with possible improvement of tensile strength of nonwovens after calendering.[23−27] It was observed that an overexposure of fabrics to the elevated temperature beyond the optimal conditions in thermal calendering of fabrics leads to failure due to fiber breakage. Below the optimum conditions, an increase in temperature or bonding time enhances fabrics strength.

In ref 22, thermal and mechanical properties of extruded sheets of soy protein with different moisture contents were studied. In particular, water adsorption was evaluated and the plasticizing effect of water was explored. The results were compared to the corresponding data for cross-linker-treated sheets. The effect of water absorption on compression-molded soy protein plastics with polyphosphate as a filler was explored in ref 28. It revealed an enhancement in water resistance and strength of specimen. In ref 29, the effect of heat treatment on tensile strength, elongation at break, and solubility in water of soy protein glycerin-plasticized films was reported. According to this research, heat-treated films became less water-soluble than the untreated films. The effect of moisture content on biodegradable films has been reported in refs 29−33. In ref 33, the effect of such plasticizers as glycerol on the water absorption properties of soy protein films was studied. It was shown that different physical and barrier properties of soy protein films can be controlled varying the content of plasticizer.

In the present work, the effect of the above-mentioned chemical cross-linking agents on tensile strength of soy-protein-containing nanofiber mats is studied. An investigation of solution-blown soy protein/nylon 6 nanofiber mats is also conducted in order to elucidate the effect of thermal bonding on tensile characteristics of nanofiber mats. We also investigate the effect of wet bonding and aging in water at an elevated temperature on mechanical properties of soy protein/nylon 6 nanofiber mats. In addition, solubility in water of the cross-linked soy protein nanofiber mats is determined. To the best of our knowledge, this is the first comprehensive study of the effect of chemical cross-linking and thermal and wet treatment on tensile strength of soy-protein-containing nanofiber mats. This work intends the utmost utilization of soy protein isolates, which are considered in many cases as agrowaste.

2. EXPERIMENTAL SECTION

2.1. Materials. Materials used in this work are as follows. Soy protein isolate [PRO-FAM 955 (SP 955)] was provided by ADM Specialty Food Ingredients. Polyamide-6 (nylon-6) (M_w = 65.2 kDa) was obtained from BASF. Formic acid (grade >95%), formaldehyde 37 wt % solution in water, A.C.S. reagent, glyoxal solution (Bioreagent ∼40% in H_2O, 8.8 M), zinc sulfate solution 0.1 mol/L in water, and sodium borohydride were purchased from Sigma-Aldrich. All materials were used as received without any further treatment and/or purification.

2.2. Solution Preparation. Blends of SPI 955/nylon 6 (40/60 and 50/50 wt/wt %) in formic acid were prepared as described in refs 5 and 6. In brief, to prepare a blend of 40/60 wt/wt % soy protein/nylon 6, 1.0 g of soy protein was added to 9.5 g of formic acid and the solution was stirred on a hot plate at 75 °C for 24 h. Then, 1.5 g of nylon 6 was added to the solution and left on a 75 °C hot plate for a day. A homogeneous solution was then ready for the solution blowing process. Similarly, to prepare a solution of 50/50 wt/wt % soy protein/nylon 6 blend, 1.5 g of soy protein 955 was mixed with 9.5 g of formic acid for 24 h on a hot plate at 75 °C. Next, 1.5 g of nylon 6 was mixed with the soy protein solution for 24 h at the same temperature. In order to produce core−shell nanofibers, core and shell solutions were prepared separately. Shell solution was 20 wt % nylon 6 in formic acid which was left on a hot plate at 75 °C for a day to stir properly. Core solution was prepared as described in refs 5 and 6. Namely, 1.3 g of SPI 955 was mixed with 8.7 g of formic acid for a day on a hot plate at 75 °C. Adding 1.0 g of nylon 6 to the solution and mixing for another day at the same temperature was the final step to prepare core solution. For solution blowing of pure nylon 6, 20 wt % solutions in formic acid were used.

2.3. Solution Blowing of Soy Protein Nanofiber Mats. To prepare soy-protein-based monolithic nanofiber mats and pure nylon 6 nanofiber mats, solution blowing[5,6] was employed. Solutions were supplied through a 13G needle. While exiting the needle, solutions were exposed to a high speed coflowing turbulent air jet with the upstream pressure of about 2.0 bar and velocity of about 150−200 m/s issued from a coannular nozzle. The solution blowing procedure was implemented at room temperature and humidity. As humidity (20−30%) in the present case was by 20−30% lower than that in ref 6, solvent evaporated faster after a solution jet was exiting the needle. Therefore, the needle-to-collector distance was reduced to 15−19 cm. Consequently, soy protein/nylon 6 monolithic nanofibers with the average diameter of 400−500 nm were formed, which corresponds to the diameter of monolithic soy protein-based nanofibers in ref 6. These nanofibers were collected and partly aligned on an aluminum rotating drum with linear velocity of about 3 m/s on the surface. Collected nanofibers formed a mat with a thickness of 0.15−0.40 mm.

Solution coblowing of core−shell nanofibers is discussed in detail in refs 5 and 6. In brief, the shell solution was supplied into a reservoir which surrounded a 18G needle issuing the core solution. The reservoir was placed on top of a 13G needle. Therefore, the core needle was located coaxially inside the shell needle. Both the core and shell solutions were supplied through the 18G and 13G needles, respectively, each with the throughput of 4 mL/h. A third annular nozzle surrounded the 18G and 13G needles, and air was issued through it coaxially with the core−shell liquid jet with the upstream pressure of about 2.0 bar. The coblown nanofibers were then collected as described above. Nanofiber mat thickness was governed by the duration of the solution blowing experiment, i.e., roughly, by the deposition time. Our previous observations[6] show that only about 50% of the mat thickness is composed of soy protein/nylon 6 nanofibers. The other 50% is the cumulative gaps between the collected layers of nanofibers. This fact is accounted for when calculating the stress acting in the mat cross-section in tensile tests.

2.4. Cross-Linking of Soy Protein Nanofiber Mats. For cross-linking, a collected nanofiber mat (50/50 SPI/nylon 6) of a certain thickness was removed from the aluminum drum. The mat was then cut into several pieces, and every single piece was weighed carefully. For chemical cross-linking, the weighed samples were immersed in a solution with a specified weight percentage of a cross-linker to the nanofiber mat. The weight

ratio of cross-linking agents to nanofiber samples was 5, 10, and 20 wt/wt %. This procedure was followed for four different types of cross-linking agents: formaldehyde, glyoxal, zinc sulfate, and sodium borohydride. After adding a cross-linking solution to the samples, open vials were left at room temperature for 24 h to dry out completely. For thermal bonding, rectangular pieces of nanofiber mats were ironed for 1 min at 55 °C. This method led to partial conglutination and cross-linking of nanofibers at the intersection points. After such treatment, nanofiber mats were left at room temperature for 15 min to cool. Prior to wet bonding, nanofiber mat samples were submerged in water and then immediately taken out. After that, wet samples with the dimensions of about 1 cm in width and 2.5 cm in length were compressed under the mass load of 150 g (i.e., under the pressure of 6 kPa) for 24 h at room temperature until they partially dried. After removing the load, these samples were left at room temperature for another day to dry out completely. Note that drying in a hood was used instead of vacuum drying, since the latter would be too fast compared with the rate of the cross-linking reactions and the samples would be either noncross-linked or partially cross-linked. It is emphasized that only samples prepared from the same batch were used for cross-linking at different concentrations to avoid variability between samples prepared from different batches. All the resulting cross-linked nanofiber mats were subjected to uniaxial tensile tests to measure the mechanical properties similarly to ref 6. In addition, solubility tests were done using samples after rapture in tensile tests, which allowed us to link solubility in water with known mechanical properties.

2.5. Heat Treatment of Cross-Linked Soy Protein/Nylon 6 Nanofiber Mats. In a different set of experiments, soy protein/nylon 6 (40/60 wt/wt %) monolithic nanofibers were cross-linked with the following three of the above-mentioned cross-linking agents: formaldehyde, glyoxal, and zinc sulfate. For each bonding agent, the cross-linking procedure in this case was conducted with four different cross-linker weight ratios to nanofiber mat: 1, 5, 10, and 50 wt/wt %. For each cross-linker concentration, one-half of nanofiber samples from a batch were heat treated after being chemically cross-linked. The second half from the same batch, which were not heat treated, were used for control. Thermal treatment was conducted as follows. After being exposed to a chemical cross-linker with a specified concentration for 24 h, the samples were left at 80 °C for 20 min on a glass slide on a hot plate. Then, mechanical properties of the heat treated cross-linked samples were compared with the control (nonheat-treated) samples from the same batch. As a result, effect of heat treatment on different covalent and ionic bonds in cross-linked samples was elucidated.

2.6. Tensile Tests of Cross-Linked Nanofiber Mats. Cross-linked soy protein/nylon 6 (40/60 and 50/50 wt/wt %) nanofiber mats were cut into rectangular shapes as described in ref 6. In brief, rectangular nanofiber mats which were 6−15 mm wide and 20−35 mm long underwent the uniaxial stretching test using Instron machine (model 5294) with 100 N capacity on pneumatic grips. The rate of stretching was kept at 1.0 mm/min for all the experiments. As a result, stress−strain behavior and mechanical properties such as Young's modulus and yield stress and maximum strain and stress at rupture (E and Y and $\varepsilon_{rupture}$ and $\sigma_{xx,rupture}$, respectively) were measured following ref 6, and the effect of different chemical cross-linking agents was investigated. For control, stress−strain curves of chemically bonded nanofiber mats were compared to those of the corresponding noncross-linked samples. As mentioned in ref 6, optical observations of solution-blown soy protein/nylon 6 nanofiber mats demonstrate that they possess a layered structure, and only 50% of a mat cross-section is filled with nanofibers. Therefore, tensile stress applied to each sample by Instron machine is only supported by a 50% cross-sectional area, which was taken into account while calculating mechanical properties.

2.7. Solubility Tests of Soy Protein Nanofiber Mats. Nanofiber samples (soy protein/nylon 6 50/50 wt/wt %) were put inside an enclosure made of a metal grid and immersed in deionized water for 24 h at room temperature. Water was constantly stirred. After the immersion, the samples were withdrawn and left at room temperature for 24 h to dry out completely. Each sample was weighed before immersion and in two days after complete drying to determine the percentage of lost weight L as

$$L = \left(1 - \frac{W_2}{W_1}\right)100\% \tag{1}$$

where W_1 is the sample weight before immersion and W_2 is the weight after immersion and drying.

2.8. Optical Observation of Cross-Linked Nanofiber Mats. All observations were done by Hitachi S-3000N variable pressure SEM, Phenom scanning electron microscope (SEM), and JEOL 6320F scanning microscope after sputter coating a 8 nm layer of Pd−Pt onto samples.

2.9. Theoretical Model. Mechanical properties of soy protein/nylon 6 monolithic and core−shell nanofibers were measured and characterized using the phenomenological model described in ref 6. For a planar strip which undergoes the uniaxial tensile test, the stress−strain dependence is given by

$$\sigma_{xx} = \sqrt{\frac{8}{3}}\, Y \tanh\left(\sqrt{\frac{2}{3}}\frac{E}{Y}\varepsilon\right) \tag{2}$$

where σ_{xx} is tensile stress and ε is tensile strain, E is Young's modulus, and Y is the yield stress. This model was used in ref 6 to predict the elastic and plastic behavior of soy/nylon 6 nanofiber mats up to the rupture point.

3. EXPERIMENTAL RESULTS AND DISCUSSION

3.1. Chemical Cross-Linking. We found that chemical cross-linking of fiber mats above 50 wt/wt % cross-linker weight ratio to nanofiber mat, led to visible macroscopic cracks in the samples. Therefore, cross-linking experiments were conducted only with 5, 10, and 20 wt/wt % ratios, except for the case of heat treatment discussed below, where 50 wt/wt % ratio was also used. The above-mentioned cracking is illustrated in Figure S1 (cf. Supporting Information) where a soy protein/nylon 6 (50/50 wt/wt %) nanofiber mat treated with 80 wt/wt % is shown. Only the cracked sample treated with glyoxal is shown, since the formaldehyde-, zinc sulfate-, and sodium borohydride-treated samples cracked similarly.

3.1.1. Cross-Linking of Soy Protein with Aldehydes and Ionic Salts. Cross-linking of soy protein with aldehydes is an example of a carbonyl−amine reaction. A detailed description of the reaction mechanism can be found in refs 16 and 34−36. In brief, chemical cross-linking can be explained as follows. In the seminal work of ref 16, it was shown that, in a wide range of pH, cross-linking starts between amino group of one amino acid with primary amide and/or guanidyl group to the other

dx.doi.org/10.1021/ie302359x | Ind. Eng. Chem. Res. 2012, 51, 15109−15121

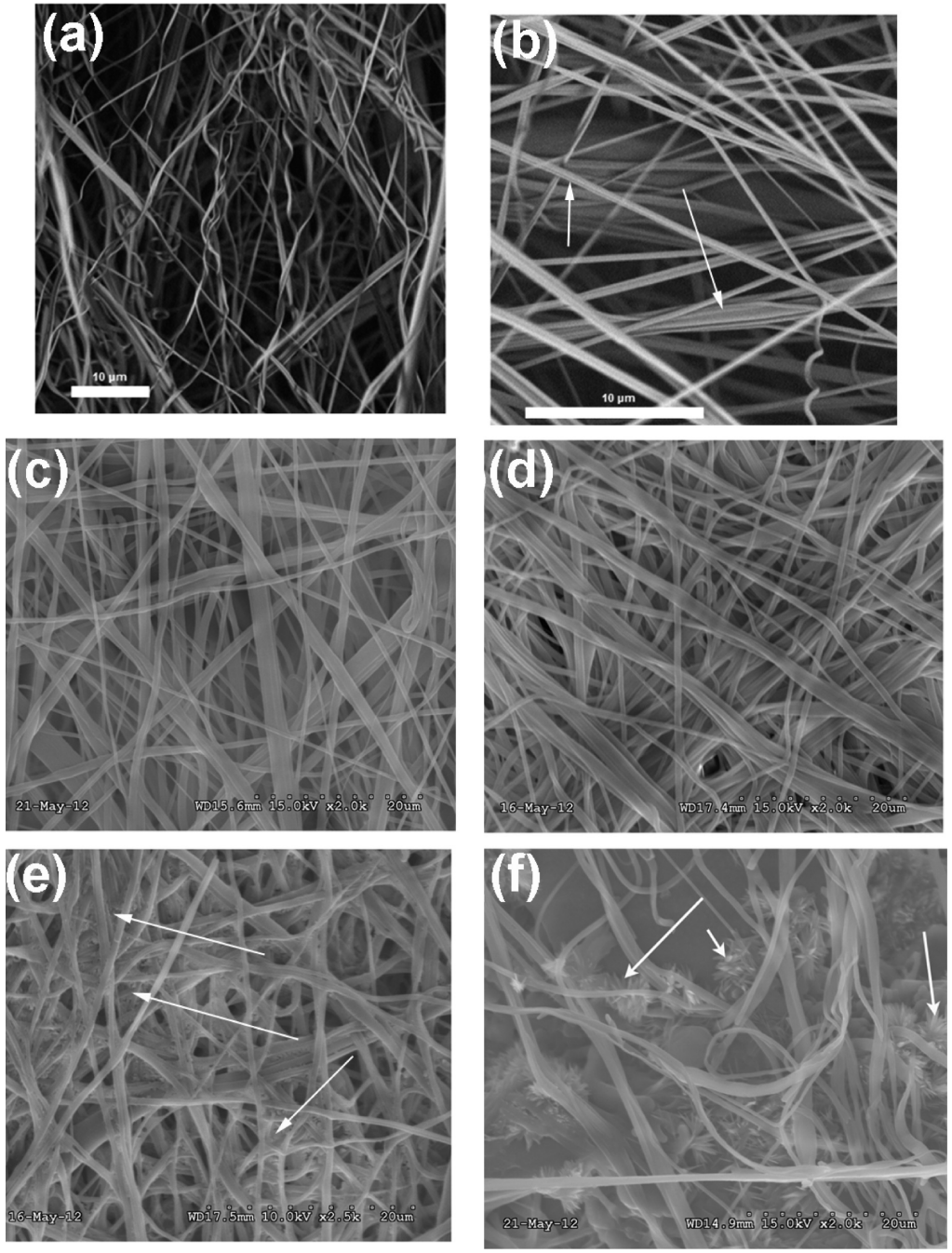

Figure 1. SEM images of pristine nanofiber mat are shown in panels (a) and (b). In panel (b), the merged nanofibers are shown by arrows. SEM images of nanofibers mat treated with 20 wt % of (c) formaldehyde, (d) glyoxal, (e) zinc sulfate, and (f) $NaBH_4$. Panel (e) reveals that there is an excessive zinc sulfate deposited on the mat as shown by arrows. Panel (f) shows that there are sharp features formed on the nanofibers mat (shown by arrows).

one under the action of aldehyde. In soy protein isolates used in the present work, the absence of aspargine and glutamine[37] implies that guanidyl groups are the potential source of cross-linking via methylene bridging. Soy protein isolate 955 used in the present work contains a very reactive lysine amino acid [~6.3% of the entire protein content[37]], which acts as the most preferential site for cross-linking due to its conformational freedom and external surface availability because of the steric effect. It is emphasized that, in addition to methylene bridging, sulfhydryl groups also participate in sulfide linkage, as it was found in ref 38. Note that the reaction kinetics reveal that complete cross-linking occurs in a time frame of 24 h.[36] That is why during cross-linking the samples were left in cross-linker solution for 24 h to facilitate complete inter- and intrafiber cross-linking. The covalent bonds thus formed restrict protein macromolecule mobility and rotation, which facilitates an increase in Young's modulus and fiber strength. A reduced flexibility of thus cross-linked protein chains makes nanofiber mats more brittle and results in reduction of strain at rupture point, $\varepsilon_{rupture}$.

Cross-linking of soy protein nanofiber mats with $ZnSO_4$ relies on metal chelation and ionic bonding. Soy protein isolates contain many polar amino acids. The addition of $ZnSO_4$ forms stable ionic bonds with these polar amino acids. In addition,

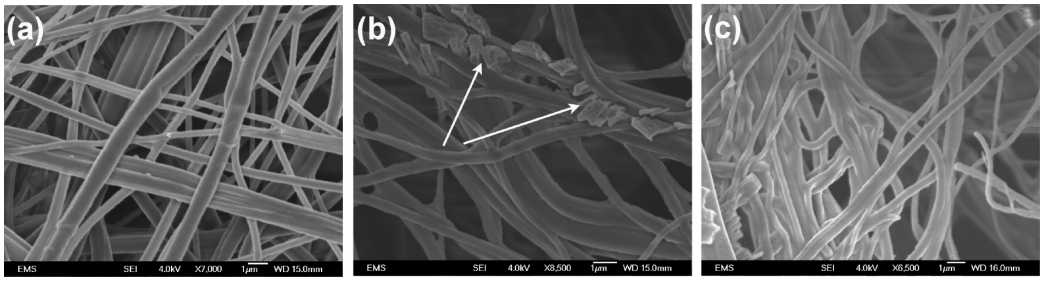

Figure 2. SEM images of nanofibers cross-linked with (a) 10 wt % zinc sulfate, (b) 10 wt % $NaBH_4$, and (c) 5 wt % $NaBH_4$. In panel (b), arrows point at the sharp features.

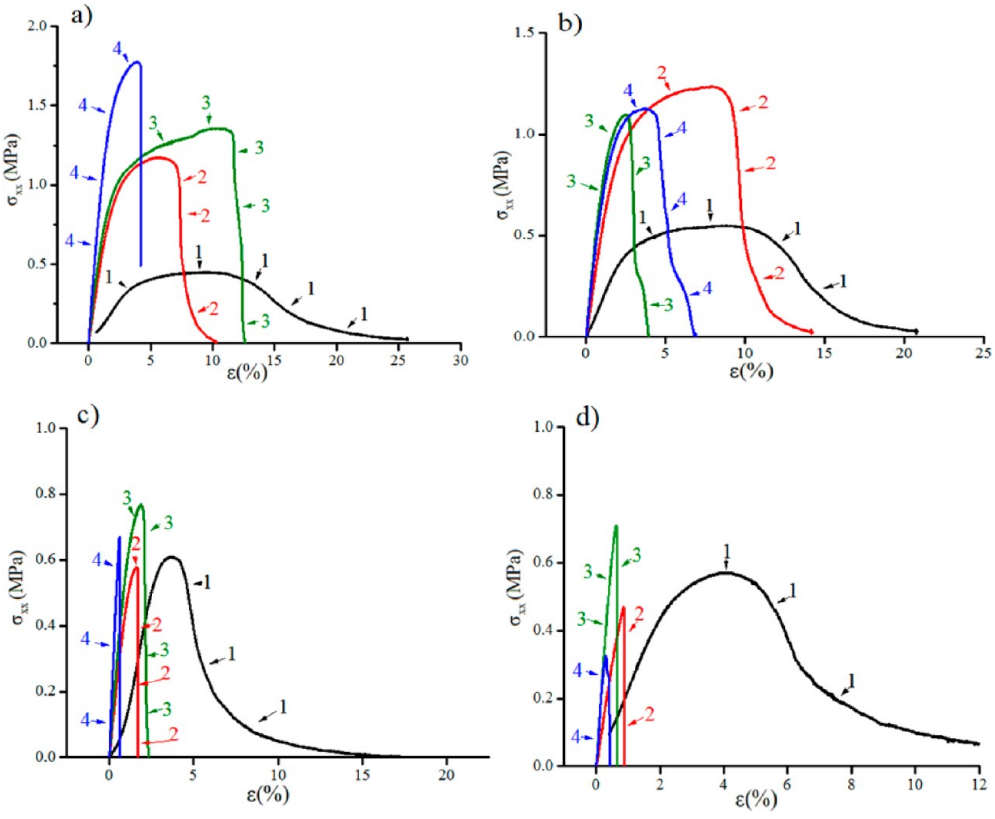

Figure 3. Stress–strain behavior of cross-linked soy protein nanofiber mats for different cross-linkers with various concentrations. In all panels, curves 1 show the stress–strain dependence for untreated soy protein nanofibers used for control, curves 2 correspond to 5 wt/wt % cross-linker/nanofiber mat ratio, curves 3 correspond to 10 wt/wt % cross-linker/nanofiber mat ratio, and curves 4 correspond to 20 wt/wt % cross-linker/nanofiber mat ratio. Panel (a) shows stress–strain behavior of soy protein/nylon 6 (50/50 wt/wt %) when formaldehyde was used as a bonding agent. In panel (b), glyoxal was used as a cross-linking agent. Panel (c) corresponds to zinc-sulfate-treated samples. Panel (d) shows sodium borohydride-treated nanofibers.

Zn^{2+} forms chelating complexes with soy protein,[21,22] which is expected to increase strength of nanofiber mats.

Sodium borohydride ($NaBH_4$) is a very strong reducing agent. Whenever protein molecules come in contact with it, the labile disulfide group containing polar amino acid (cystine) is attacked, which results in sulfhydryl–disulfide exchange. This, in turn, results in opening up of the inter- and intramolecular disulfide bonds, which are readily oxidized by air and cross-linked across the chain.[39]

3.1.2. SEM Images of Cross-Linked Nanofiber Mats. SEM images of a pristine solution-blown nanofiber mat are shown in Figure 1a,b, and of cross-linked samples with 20 wt % of the cross-linkers are shown in Figure 1c–f. In particular, Figure 1c–f shows SEM images of the samples treated with formaldehyde, glyoxal, zinc sulfate, and sodium borohydride, respectively. The SEM images of the noncross-linked nanofibers (Figure 1b) show that the fibers merged together at several places shown by arrows. This stems from the fact that, when nanofibers are collected on the rotating drum, they still remain semiwet and can merge. The degree of merging is higher when the relative humidity is higher. It can be seen that, for the organic cross-linkers, formaldehyde (Figure 1c) and glyoxal (Figure 1d), nanofiber morphology does not change and there is no deposit or film formed. These observations show that reaction between nanofiber mats and the organic cross-linkers were completed. However, for the ionic cross-linker, zinc sulfate (Figure 1e), there are visible deposits of zinc sulfate on nanofibers (shown by arrows) in comparison to the noncross-linked fibers (Figure 1a,b), which shows that an excessive cross-linker was left. It can be also seen that at some

dx.doi.org/10.1021/ie302359x | *Ind. Eng. Chem. Res.* 2012, 51, 15109–15121

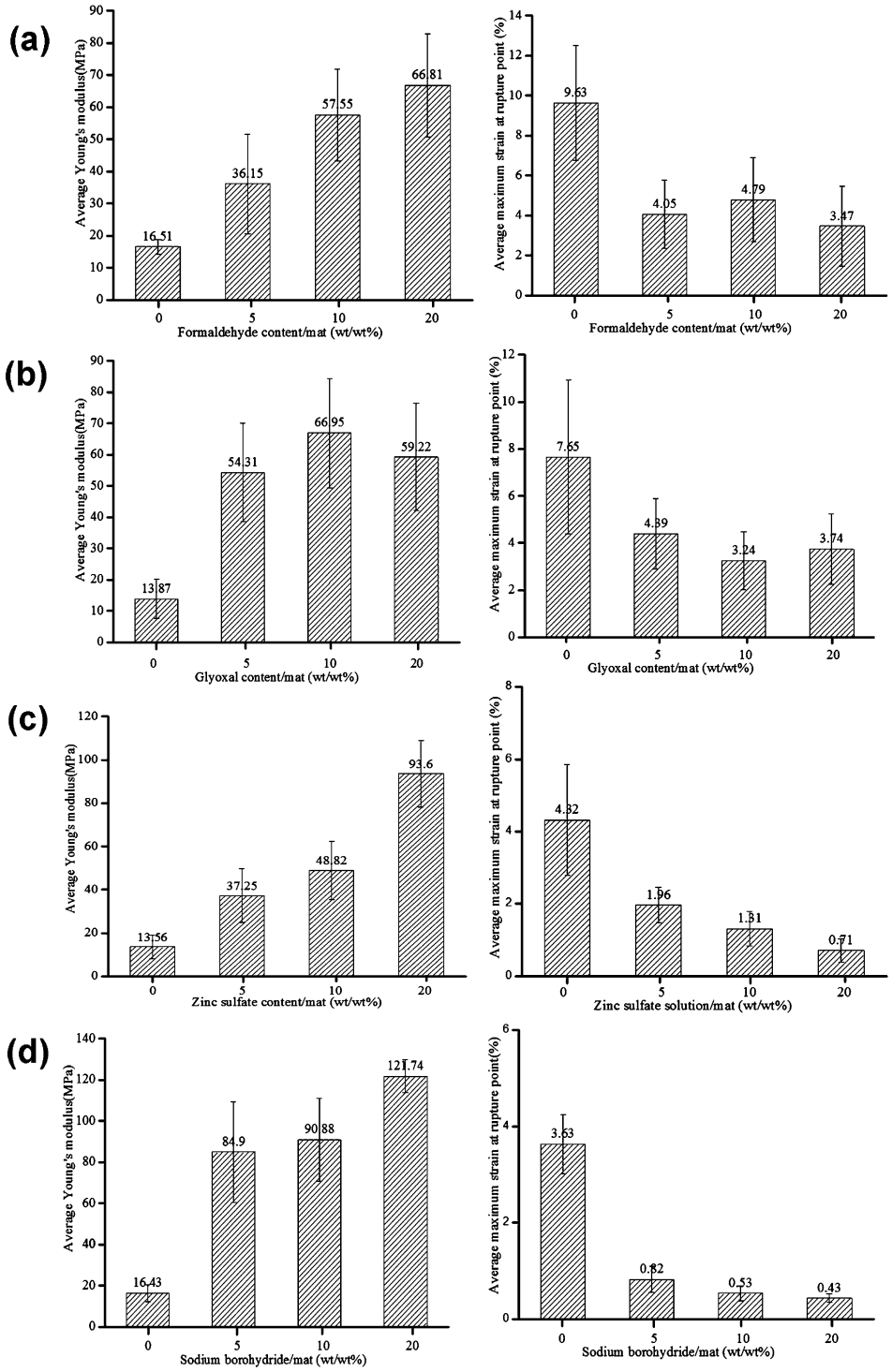

Figure 4. Average Young's modulus and maximum strain at rupture for the same batch of cross-linked soy protein samples at different concentrations of (a) formaldehyde, (b) glyoxal, (c) zinc sulfate, and (d) sodium borohydride used as cross-linkers. Fiber mats revealed lower plasticity as the cross-linker content increased.

places the nanofibers got fused. This can stem from two different facts. (i) As shown in Figure 1b, the semiwet pristine nanofibers could be merged, or (ii) an additional merging could occur since soy protein is partially soluble in water. However, it is emphasized that most of the nanofibers were not fused or merged as is shown in Figure 2a, where although the zinc sulfate concentration is low (10 wt/wt %) and, thus, water content is higher, there is no such merger visible. It means that in most of the cases there was no fiber dissolution. For $NaBH_4$ (Figure 1f), it is seen that there are some sharp crystalline features visible on nanofibers (shown by arrows), which means that a higher than 20 wt % mass ratio of the ionic cross-linker would be definitely too much. It was found that, when the mass ratio of zinc sulfate was decreased to 10 wt %, there was no more deposits on nanofibers anymore (Figure 2a). However, for $NaBH_4$, it was found that, even at 10 wt % mass ratio, some nanofibers with fewer sharp features were still visible (Figure 2b). Only when the mass ratio of $NaBH_4$ was reduced to 5 wt

dx.doi.org/10.1021/ie302359x | Ind. Eng. Chem. Res. 2012, 51, 15109−15121

%, these features practically disappeared (Figure 2c). To resolve the chemical nature of these sharp structures, the elemental analysis was done on a nanofiber mat treated with 10 wt % $NaBH_4$. Two different places were used: the smooth part and the rough patches (shown by two arrows in Figure 2b). In these experiments, Hitachi S-3000N variable pressure SEM was used. It was found that at both places the amount of sodium was comparable (~6−8% of the total signal in both cases). If the sharp features were only composed of the excessive $NaBH_4$, the elemental analysis would have shown higher amounts of sodium there compared with the smooth fiber part. Comparable amounts of sodium at both locations clearly show that the reaction is complete. Therefore, these sharp features are most probably remnants of broken pieces caused by handling. This conclusion is supported below by the results of the tensile tests, which show that cross-linking with $NaBH_4$ made nanofiber mats most brittle.

3.1.3. Stress−Strain Curves of Cross-Linked Soy Protein Nanofiber Mats. Figure 3a−d illustrates the typical stress−strain dependences of soy protein/nylon 6 (50/50 wt/wt %) nanofiber mats after cross-linking in the presence of 5, 10, and 20 wt/wt % of different cross-linkers. It is seen that sodium borohydride and zinc sulfate mostly affected the strength of nanofiber mats, whereas the samples treated with formaldehyde and glyoxal show more plastic behavior than those treated with $NaBH_4$ and $ZnSO_4$. This clearly demonstrates that the ionic agents were more effective in cross-linking in comparison to the aldehydes, which will be discussed in more detail in the following sections.

It is emphasized that noncross-linked samples from different batches were used in Figure 3a−d. Even though they result in almost the same Young's modulus values, their maximum strain at rupture varies significantly (cf. Figure 4) due to variability of the process, namely, the interfiber bonding, relative humidity, etc.

3.1.4. Mechanical Properties of Soy Protein Nanofibers Cross-Linked Using Formaldehyde. While using formaldehyde as a cross-linker, it was found that an addition of formaldehyde resulted in an increase in Young's modulus of soy protein nanofiber mat and reduction of strain at rupture ($\varepsilon_{rupture}$) compared to the corresponding noncross-linked samples (Table S1 in Supporting Information and Figure 4a). The maximum increase in Young's modulus corresponded to the ratio of 20 wt/wt % of cross-linker to nanofiber mat in the cross-linking process. The mechanical properties of formaldehyde-cross-linked samples are listed in Table S1 (cf. Supporting Information). Average Young's modulus of noncross-linked soy protein/nylon 6 nanofiber mats was measured as 16.51 ± 2.39 MPa, whereas the value of 66.81 ± 16.05 MPa was achieved for the ratio of 20 wt/wt % of formaldehyde to nanofiber mat. In addition, maximum strain at rupture for the noncross-linked samples is reported as 9.63 ± 2.88%. In the present work, the maximum strain at rupture was reduced to 3.47 ± 2.00% for the formaldehyde-cross-linked samples with 20 wt %/wt% cross-linker/nanofiber mat ratio. An increase in formaldehyde content in the cross-linking process resulted in a lower strain at rupture, which implies a reduced plasticity of the cross-linked nanofiber mats. Consequently, lower plasticity observed in samples cross-linked with a higher than 20 wt/wt % formaldehyde mass ratio resulted in noticeable ruptures while drying at room temperature. Therefore, tensile tests could not be conducted with these samples. The average Young's modulus of comparable pure nylon 6 solution-blown nanofiber mats is 8.59 ± 0.88 MPa. Therefore, chemically modified soy protein nanofiber mats with formaldehyde used as a cross-linker reveal a higher Young's modulus than for the corresponding pure nylon 6 nanofiber mats.

3.1.5. Mechanical Properties of Soy Protein Nanofibers Cross-Linked Using Glyoxal. The effect of glyoxal as a cross-linker is specified in Table S1 (cf. Supporting Information) and Figure 4b. The glyoxal/mat weight ratio in the cross-linking process varied in the range of 0−20 wt/wt %. Young's modulus and yield stress increased with glyoxal percentage up to 10 wt/wt %. It can be seen that using glyoxal as a cross-linker led to Young's modulus of soy protein nanofiber mats almost 5 times higher than that of the noncross-linked samples, which is reported as E = 13.87 ± 6.36 MPa (Table S2 in Supporting Information). In the present work, Young's modulus of glyoxal-cross-linked soy protein nanofiber mats reached E = 66.95 ± 17.48 MPa for 10 wt/wt % cross-linker/nanofiber mat ratio. The average maximum strain at rupture reported as 7.65 ± 3.26% for the noncross-linked samples was reduced to 3.24 ± 1.23% for 10 wt/wt % glyoxal/nanofiber mat ratio in the cross-linking process. This result reveals an increased brittleness of nanofibers due to cross-linking with glyoxal. Increasing glyoxal content above 20 wt/wt % in the cross-linking process did not further improve mechanical properties of the samples due to high brittleness. It led to observable cracks in the nanofiber mat structure. These cracks resulted in fragile nanofiber samples.

Comparison of the data for glyoxal cross-linking listed in Table S1 (cf. Supporting Information) with those for the formaldehyde cross-linking in Table S1 (cf. Supporting Information) shows that the former results in higher values of Young's modulus E than the latter up to the cross-linker mass ratio of 20 wt/wt %. It is emphasized that, in the case of formaldehyde, the E value increased monotonically with an increase in the content of formaldehyde. On the contrary, in the case of glyoxal, the E value increased up to 10 wt/wt % of glyoxal and then decreased when the mass ratio increased to 20 wt/wt % of glyoxal. Also, the strain at rupture is lower in the case of glyoxal compared to that of formaldehyde. References 40 and 41 report values comparable to our values of E in solid extruded sheets cross-linked using glyoxal and formaldehyde.

The higher stiffness achieved using glyoxal compared to that with formaldehyde up to 10 wt/wt % can be explained as follows. Both glyoxal (OCHHCO) and formaldehyde (HCHO) have aldehyde groups. However, glyoxal has more available aldehyde groups facilitating more cross-linking sites than formaldehyde, which results in a higher strength of glyoxal-cross-linked nanofiber mats compared to the formaldehyde-treated ones. Note also that nanofiber mats subjected to cross-linking are porous fluffy materials in distinction from the solid extruded sheets cross-linked in refs 40 and 41. The open porosity of nanofiber mats resulted in an easier cross-linker access and high E values comparable to those of solid sheets in refs 40 and 41.

Table S1 (cf. Supporting Information) also reveals that Young's modulus E reached the maximum values for the cross-linker/nanofiber mat ratio in the cross-linking process in the range of 10−20 wt/wt %. In the case of formaldehyde, it can be seen that an increase in its content in the range of 10 to 20 wt/wt % did not result in any appreciable change in the value of E, as it did in the range of 5−10 wt/wt %. In the case of glyoxal, the mean value of E corresponding to 20 wt/wt % of glyoxal decreased as compared to that for 10 wt/wt %. One can speculate, as in ref 40, that an increase in the cross-linker

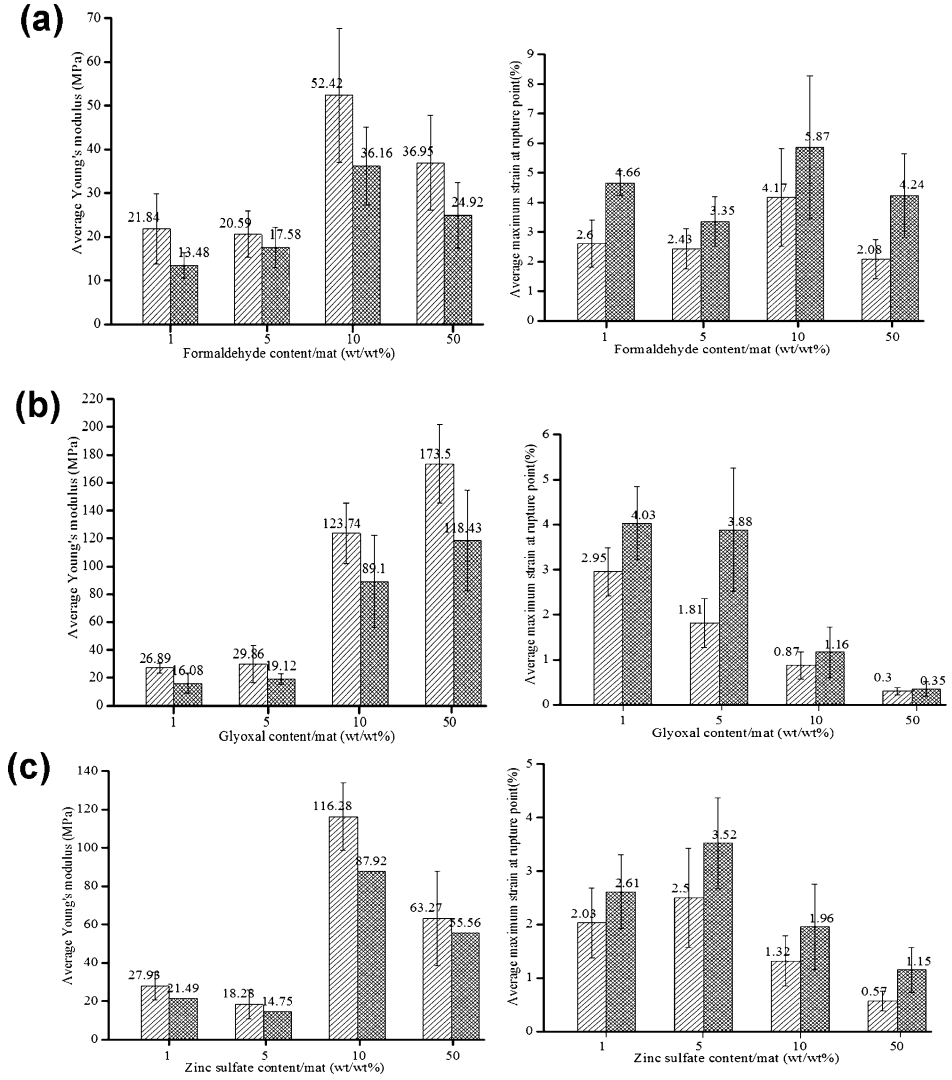

Figure 5. Young's modulus and the average maximum strain at rupture for both thermally treated and untreated soy protein/nylon 6 nanofiber mats (40/60 wt/wt %) which were cross-linked using: (a) formaldehyde, (b) glyoxal, and (c) zinc sulfate solutions. Right columns correspond to the cross-linked nanofiber mats that were heat treated for 20 min at 80 °C on a glass slide left on a hot plate. Left columns illustrate the data for the cross-linked nanofiber sample which were not exposed to any heat treatment. A decrease in the average Young's modulus of heat-treated samples (right columns) results from the fact that covalent or ionic bonds are destroyed while being heated. In panel (a), the maximum strain at rupture for both thermally treated samples and those which did not undergo heat treatment was found at 10 wt/wt % formaldehyde/nanofiber mat ratio. In panel (b), as glyoxal percentage in the cross-linking process increased, the sample brittleness increased, which corresponds to the diminished values of $\varepsilon_{rupture}$. However, at those glyoxal concentrations, the plasticizing effect of heat treatment is small. Panel (c) illustrates the results for the ionically bonded nanofibers when zinc sulfate solution was used. As the zinc sulfate content in the chelation process increases beyond 5%, the sample brittleness increases as well, which results in lower values of $\varepsilon_{rupture}$. Note that the plasticizing effect of heat treatment is lower for higher contents of zinc sulfate.

content might have plasticized the samples. However, Table S1 (cf. Supporting Information) shows that, as the cross-linker/nanofiber mat ratio increased, the strain at rupture decreased. This shows that the cross-linkers did not plasticize the samples at higher concentrations. The reduction in the value of E at the higher cross-linker mass ratios can be attributed to the fact that, as the aldehyde content was increased, the number of possible inter- and intrafiber linkages between protein chains also increased. Therefore, the material became overstretched and microcracks appeared. This resulted in an earlier rupture and lowered strength, as revealed experimentally.

3.1.6. Mechanical Properties of Soy Protein Nanofibers Treated Using Zinc Sulfate. Effect of cross-linking with $ZnSO_4$ is shown in Table S1 (cf. Supporting Information). It can be seen that adding zinc sulfate solution to soy protein nanofiber mats resulted in about a 7 times increase in the average Young's modulus of samples which were cross-linked at 20 wt/wt % zinc sulfate/nanofiber mat ratio compared to untreated samples. As nanofiber mats became stronger due to the effect of the ionic bonding agent, brittleness of the mats became more considerable. Reduction of the maximum strain at rupture from 4.32 ± 1.54% for noncross-linked samples to 0.71 ± 0.32% for those cross-linked at 20 wt/wt % zinc sulfate/nanofiber mat ratio clearly shows that. Table S1 (cf. Supporting Information) demonstrates that cross-linking with $ZnSO_4$ has a stronger effect compared to aldehyde compounds. Figure 4c shows the overall trends for soy protein/nylon 6 mats, in

dx.doi.org/10.1021/ie302359x | Ind. Eng. Chem. Res. 2012, 51, 15109−15121

Table 1. Weight Loss Data for 50/50 wt/wt % Soy Protein/Nylon 6 Monolithic Nanofiber Mats (Cross-Linked and Noncross-Linked) and Core-Shell Nanofiber Mats[a]

soy protein/nylon 6 nanofiber samples	average weight loss (%)	soy protein/nylon 6 nanofiber samples	average weight loss (%)
monolithic noncross-linked	21.85	core−shell noncross-linked	5.28
monolithic 5 wt/wt % glyoxal cross-linked	19.97	monolithic 5 wt/wt % zinc sulfate cross-linked	15.48
monolithic 10 wt/wt % glyoxal cross-linked	21.80	monolithic 10 wt/wt % zinc sulfate cross-linked	24.60
monolithic 20 wt/wt % glyoxal cross-linked	17.07	monolithic 20 wt/wt % zinc sulfate cross-linked	28.29
monolithic 5 wt/wt % formaldehyde cross-linked	17.05	monolithic 5 wt/wt % sodium borohydride cross-linked	18.32
monolithic 10 wt/wt % formaldehyde cross-linked	16.65	monolithic 10 wt/wt % sodium borohydride cross-linked	17.94
monolithic 20 wt/wt % formaldehyde cross-linked	23.65	monolithic 20 wt/wt % sodium borohydride cross-linked	15.51

[a]Samples were left in water for 24 h at room temperature.

particular, in Young's modulus and maximum strain at rupture at different zinc sulfate contents.

3.1.7. Mechanical Properties of Soy Protein Nanofibers Treated Using Sodium Borohydride. Tensile tests were also conducted with soy protein/nylon 6 samples which were cross-linked using sodium borohydride. Table S1 (cf. Supporting Information) demonstrates that the maximum strength for such nanofiber samples was achieved at 20 wt/wt % cross-linker/nanofiber mat ratio. As with the other types of cross-linkers, stronger nanofiber mats were less plastic. Using sodium borohydride resulted in almost 7 times stronger nanofiber mats compared to the untreated ones (cf. Table S1 in Supporting Information and Figure 4d).

Both zinc sulfate and sodium borohydride had the strongest effect on the soy protein nanofiber strength compared to the same formaldehyde- or glyoxal-to-nanofiber mat ratio. Therefore, stronger protein−protein interactions were achieved in nanofiber mats that were chemically treated with sodium borohydride and zinc sulfate solutions. This implies that ionic bonds formed between polymeric chains in protein structure are stronger than inter- and intramolecular bonds formed by covalent cross-linking agents.

3.1.8. Effect of Heat Treatment on Cross-Linked Soy Protein Nanofiber Mats. Cross-linked soy protein/nylon 6 nanofiber mats were heated up to 80 °C for 20 min. This was done to reveal the effect of heat treatment on the cross-linked nanofiber mats for different cross-linkers used at different contents. Figure 5 shows the average Young's modulus of soy protein nanofiber samples as a function of cross-linker content for three different agents used for nanofiber treatment: formaldehyde, glyoxal, and zinc sulfate solution. In each case, the average Young's modulus of thermally treated and untreated cross-linked samples are compared for each cross-linker content. Figure 5 shows that the average Young's modulus of the heat-treated cross-linked samples is lower compared to Young's modulus of comparable untreated samples.

It was shown in refs 18, 22, and 42 that heat treatment of chemically noncross-linked proteins results in stronger inter- and intramolecular cross-linking mostly between cystine and lysine amino acids owing to the presence of the labile disulfide bond, which results in a higher Young's modulus and lower strain at rupture. This effect is, in part, due to the fact that heated samples contain less moisture. Therefore, an inevitable plasticizing effect of water is reduced due to heat treatment, and heat-treated samples reveal a higher Young's modulus and appear to be more brittle. Note also that, if noncross-linked nanofiber mats were subjected to heat treatment, nylon 6 present in the samples would soften (the glass transition temperature of nylon varies between 47 and 57 °C[43]) and conglutinate nanofibers at certain locations. Such conglutination should result in an increase in strength of the heat-treated noncross-linked nanofiber mats, as it is shown below. Note that it was shown that heating cleaves the methylene bridges for aldehyde-fixated proteins.[44,45] It was also shown that, when chelated complex of chitin with zinc was heated, the release of zinc in water becomes higher, which clearly shows that heat treatment results in cleavage of the chelated complex.[46] Therefore, it is expected that, for the chemically cross-linked samples subjected to heat treatment, the inter- and intraprotein linkages formed by covalent or chelated and ionic bonds will break. It is also expected that, when heat source will be removed and the samples cooled to room temperature, the broken bonds cannot restore themselves completely. This is because after heat treatment when the cross-linkers are in their "frozen" state, they lose their mobility and cannot cross-link the protein with the same efficacy as they do in solution. As a result, for the thermally broken bonds, it is energetically favorable to form bonds with the nearest possible amino acids instead of the "exotic" linkages formed by the cross-linkers before the heat treatment. This results in an increased flexibility at an expense of the lowered strength in spite of conglutination of nylon-6 in the soy protein nanofiber mats as mentioned before.

As the amount of cross-linking agent in the cross-linking process increased, nanofiber mats in most cases became more brittle. The heat treatment of the cross-linked samples tends to diminish this effect as is seen in Figure 5, as expected according to refs 44−46 and the discussion in the previous paragraph. As a result of heat treatment, some cross-linked sites are broken and protein chains recover their mobility, which makes nanofiber mats more plastic. A detailed comparison of the average mechanical properties of heat-treated and nonheat-treated samples which were cross-linked with different agents is presented in Table S2 (cf. Supporting Information).

3.1.9. Water Solubility of Soy Protein Nanofiber Mats. Following eq 1, water solubility of soy protein/nylon 6 (50/50 wt/wt %) nanofiber samples, which were modified with different cross-linking agents, was investigated. Water-solubility test data for monolithic noncross-linked samples and those monolithic samples that were chemically bonded using various agents are reported in Table 1. The table also contains results for core−shell soy protein/nylon 6 nanofiber mats (without any cross-linking). It can be seen that core−shell soy protein/nylon 6 nanofiber samples revealed a significantly lower weight loss in water compared to either cross-linked or noncross-linked samples. Since soy protein is in the core and protected by nylon 6 in the shell, such core−shell nanofibers possess an enhanced water longevity compared to all monolithic fibers (cross-linked or not). Overall, among the monolithic nano-

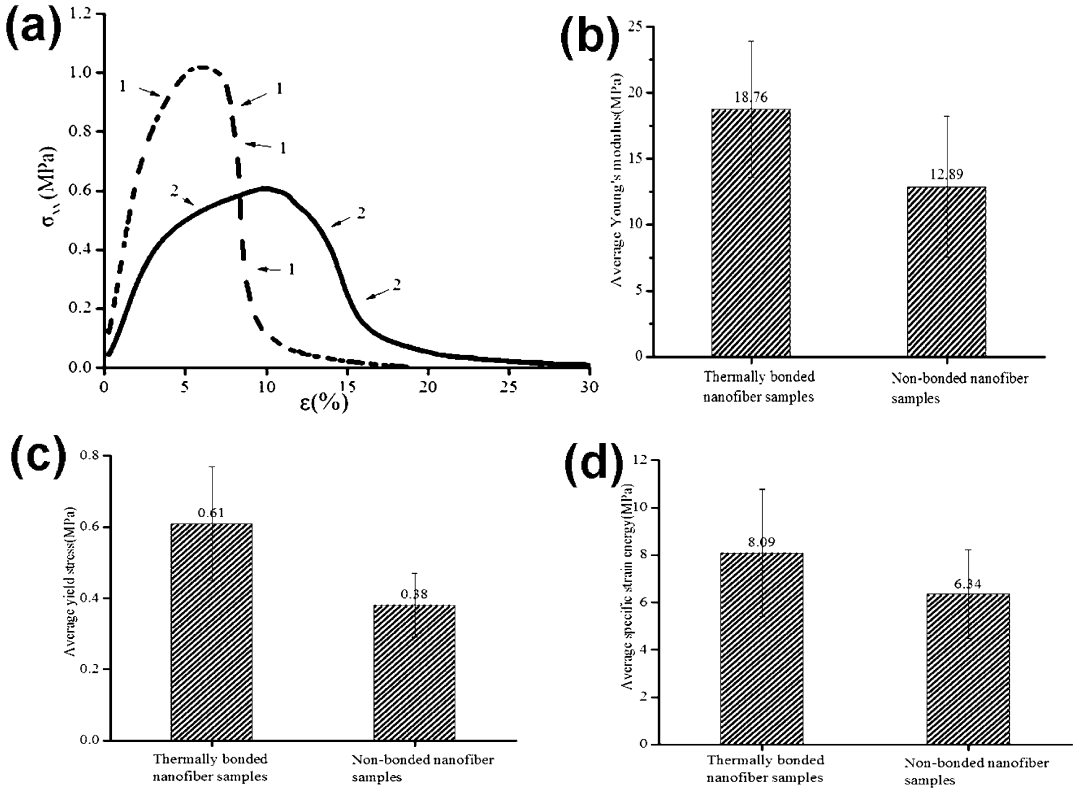

Figure 6. Comparison of thermally bonded and nonbonded samples. Panel (a) shows the stress−strain curves of soy protein/nylon 6 (40/60 wt/wt %) nanofiber mats: curve 1, thermally bonded (at 55 °C under compression) nanofiber mat; curve 2, nonbonded nanofiber mat. The normal stress in the stretching direction is denoted σ_{xx}; the tensile strain is ε (%). Panel (b) shows the average Young's modulus. Panel (c) shows the average yield stress, and panel (d) shows the average specific strain energy. The average Young's modulus, the yield stress, and specific strain energy increase when nanofiber samples are exposed to heat treatment.

fibers, the cross-linked samples did not show a much different weight loss than the noncross-linked samples. For comparison, in ref 44, cast soy protein isolate films were left in a 50 mL beaker for 24 h at 25 °C, which resulted in 28.69 ± 1.1% of material loss.

3.2. Physical Cross-Linking. *3.2.1. Thermal Bonding.* The rectangular samples were used in tensile tests in order to reveal their stress−strain characteristics. Figure 6a compares stress−strain curves for samples of soy protein/nylon 6 (40/60 wt/wt %) nanofiber mats which underwent the bonding process described above with those which did not (taken from the same batch of samples). It is clearly seen that thermal bonding increases Young's modulus, the yield stress, and tensile stress of soy-protein-containing nanofiber mats. The corresponding average data are combined in Figure 6b−d, for Young's modulus E, the yield stress Y, and the specific strain energy $U = \int_0^{\varepsilon} \sigma_{xx}\, d\varepsilon$. The cumulative data for all the measured parameters is presented in Table S3 (cf. Supporting Information). The average Young's modulus of nontreated nanofiber mats was found as 12.89 ± 5.34 MPa. The nanofiber mat strength increased to 18.76 ± 5.17 MPa after heat treatment under compression for only 1 min. When exposed to heat treatment, nylon 6 present in the samples softens and forms conglutination points, which result in physical cross-linking of nanofibers and an increase in the average Young's modulus. Also, it was observed that samples became more brittle after heat treating. The original average maximum strain at rupture $\varepsilon_{rupture}$ for soy protein nanofiber mats was found as 8.19 ± 1.71%, whereas the ironing of the samples at 55 °C for 1 min resulted in $\varepsilon_{rupture}$ of 6.86 ± 1.17%.

3.2.2. Wet Bonding. The dried samples underwent uniaxial tensile test using Instron, and their stress−strain curves were measured. As a result, the effect of wet conglutination under a load was evaluated. This effect stems from the interfiber conglutination in the wet state at the intersection points. Indeed, soy protein isolate used in the present work is partially soluble in water. In wet state at the intersection points, soy protein of different nanofibers merged and formed bonds on drying.

It was found that, due to the wet conglutination and the resulting cross-linking effect, the overall mechanical properties of soy-protein-containing nanofiber mats were enhanced. Young's modulus showed an increase of about 65%, which can be attributed to bonds formed at the wet intersection points. As a result, the specific strain energy U increased by approximately 33%. The average yield stress stayed practically unchanged. However, after wet treating, nanofiber mats were also plasticized, as both soy protein isolate and nylon 6 absorb water. That is the reason that the strain at breakup does not decrease although the strength increases. Figure 7 and Table S4 (cf. Supporting Information) compare the average mechanical properties of the prewetted and wet-conglutinated nanofibers with those of the corresponding untreated samples. Figure S2 (cf. Supporting Information) shows the SEM images of the soy protein/nylon 6 (40/60 wt/wt %) nanofibers after they were prewetted and wet-conglutinated under the load of 150 g. The images in Figure S2 (cf. Supporting Information) demonstrate that after the wet conglutination under load the individual nanofibers keep their individuality.

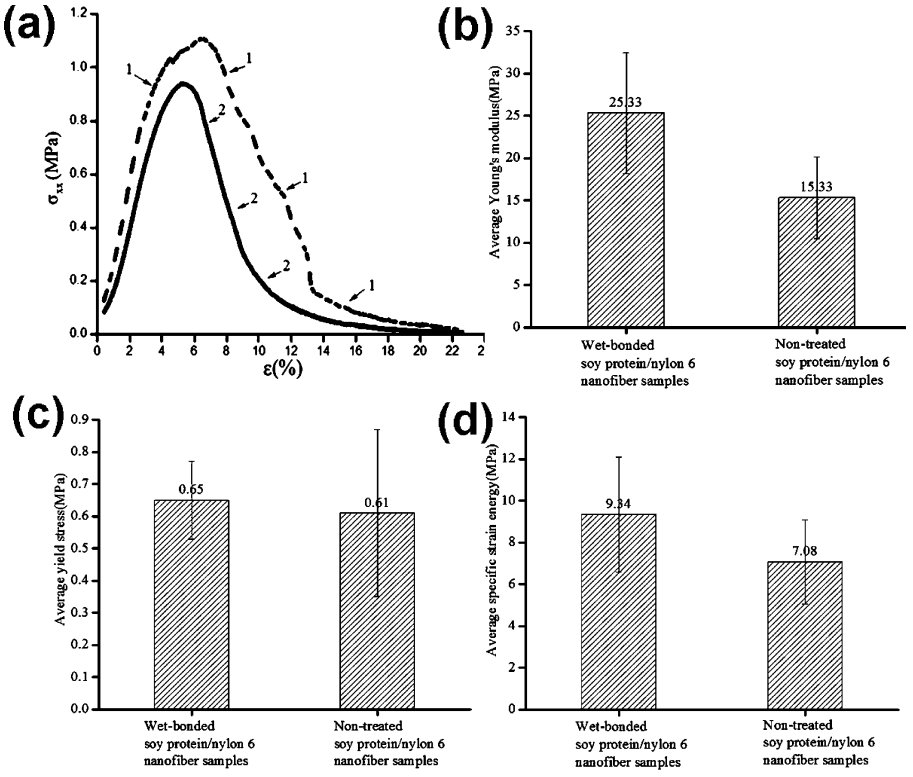

Figure 7. Comparison of prewetted, wet-conglutinated and nontreated samples. Panel (a): curve 1 shows the stress−strain curve of a prewetted, wet-conglutinated nanofiber sample under 150 g load. The stress−strain curve of the corresponding nontreated nanofiber sample from the same batch is shown as curve 2. It can be seen that the wet-conglutinated sample reveals a higher Young's modulus and specific strain energy compared to the untreated one. Panel (b) shows the average Young's modulus; panel (c) shows the average yield stress, and panel (d) shows the average specific strain energy.

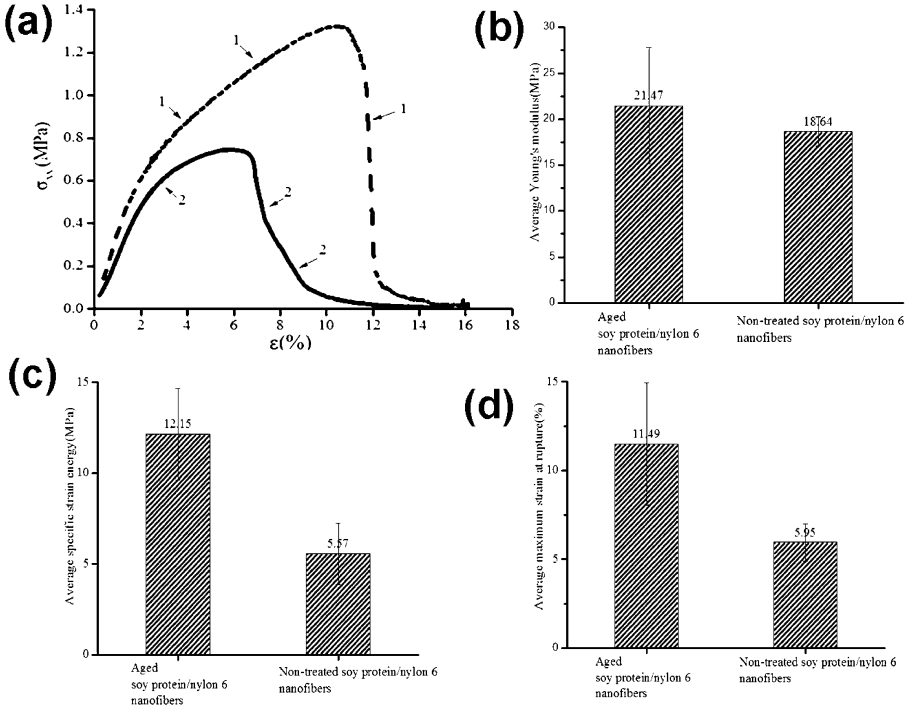

Figure 8. Comparison of humid-aged and nontreated samples. (a) Stress−strain curve for a humid-aged (in hot water) soy protein nanofiber sample is shown as curve 1. The stress−strain curve for the corresponding untreated sample is shown as 2. Significantly higher values of Young's modulus and specific strain energy were found for the humid-aged nanofiber samples. (b) The average Young's modulus, (c) specific strain energy, and (d) maximum strain at rupture of soy protein/nylon 6 (40/60 wt/wt %) nanofiber mats aged in hot water for 1 h compared to those of the corresponding nontreated samples.

dx.doi.org/10.1021/ie302359x | *Ind. Eng. Chem. Res.* 2012, 51, 15109−15121

3.2.3. Humid Aging Test. The humid aging of soy protein nanofiber mats was explored as follows. Nanofiber samples were left in water at 80 °C for 1 h. After that, the samples were extracted from water and left at room temperature for 24 h to dry out without applying any pressure. Then, the samples were used in tensile tests. This experiment reveals the mechanical properties of soy protein/nylon 6 nanofiber mats after the exposure to severe humidity conditions and elevated temperature. A typical stress−strain curve for humid-aged nanofibers after their immersion in hot water for 1 h is depicted in Figure 8a, where the stress−strain curve is compared with the one for the corresponding nontreated sample.

The results obtained for the humid-aged samples demonstrate the effect of wet aging in hot water on soy protein nanofiber mats. An increase of about 16% in Young's modulus and doubled specific strain energy were recorded. On the other hand, the yield stress practically did not change (cf. Figure 8b−d and Table S5 in Supporting Information). The mechanical properties of the humid-aged nanofiber samples are compared with those for the corresponding untreated samples in Figure 8b−d. In particular, Figure 8d and Table S5 (cf. Supporting Information) illustrate an enhanced plasticity range of humid-aged nanofiber mats. The maximum strain at rupture ($\varepsilon_{rupture}$) is reported as 5.95 ± 1.04 for untreated samples, whereas this parameter increased to 11.49 ± 3.44 for nanofiber mats after the humid-aging experiment. Therefore, it is shown that, while soy protein-containing nanofiber mats retained their strength under the conditions of the extreme humidity and temperature, they were also significantly plasticized compared to the original samples.

4. CONCLUSION

The experiments were conducted using two methods of cross-linking of soy-protein-containing nanofiber mats, namely, chemical and physical methods. In chemical cross-linking, two covalent cross-linkers (formaldehyde and glyoxal) and two ionic cross-linkers (zinc sulfate and sodium borohydride) showed that these cross-linkers can increase nanofiber mat strength almost 3−4, 5, 7, and 7 times, respectively. It is emphasized that only samples that were prepared from the same batch collected on a rotating drum were used in tensile tests of the noncross-linked and cross-linked nanofiber mats to minimize the effect of the process variability. Then, for any cross-linked and noncross-linked samples, tensile tests were conducted several times and that established the reported values of Young's modulus and strength. As an increase in 3−7 times is observed in comparison of the cross-linked to noncross-linked samples, it cannot be attributed to the process variability, i.e., to fiber diameter, porosity, interconnections, etc., varying from batch to batch.

The results show that ionic bonding in soy protein structure results in the higher Young's modulus compared to the aldehyde-treated fibers. Heat treatment mostly plasticizes the cross-linked nanofiber mats. In the experiments on mass loss in water, it was shown that the best longevity is achieved with core−shell nanofiber mats, where soy protein is located in the core.

In physical cross-linking, thermal bonding of nanofibers under compression led to an almost 50% increase in Young's modulus, as well as a slight enhanced brittleness of the samples. Prewetting and wet conglutination under 6 kPa load resulted in samples with Young's modulus of almost 65% higher than that for the corresponding nontreated ones. The higher maximum strain at rupture of humid-aged nanofiber mats is indicative of plasticizing effect of water.

■ ASSOCIATED CONTENT

Ⓢ Supporting Information

Image of soy protein/nylon 6 (50/50 wt/wt %) nanofiber mat cross-linked at 80 wt/wt % glyoxal/nanofiber mat ratio, SEM images of soy protein/nylon 6 nanofibers after prewetting and wet conglutination under the load of 150 g, and tables showing mechanical properties of soy protein nanofibers cross-linked with different cross-linkers. This material is available free of charge via the Internet at http://pubs.acs.org.

■ AUTHOR INFORMATION

Corresponding Author

*E-mail: ayarin@uic.edu. Tel.: (312) 996-3472. Fax: (312) 413-0447.

Notes

The authors declare no competing financial interest.

■ ACKNOWLEDGMENTS

This work was supported by a research contract with the United Soybean Board, Chesterfield, Missouri (research Contract No. 0491).

■ REFERENCES

(1) Kaplan, D. L. *Biopolymers from renewable resources*; Springer: Berlin, 1998.

(2) Liu, D.; Chen, H.; Chang, P. R.; Wu, Q.; Li, K.; Guan, L. Biomimetic soy protein nanocomposites with calcium carbonate crystalline arrays for use as wood adhesive. *Bioresour. Technol.* **2010**, *101*, 6235.

(3) Ciannamea, E. M.; Stefani, P. M.; Ruseckaite, R. A. Medium-density particleboards from modified rice husks and soybean protein concentrate-based adhesives. *Bioresour. Technol.* **2010**, *101*, 818.

(4) Zoppe, J. O.; Peresin, M. S.; Habibi, Y.; Venditti, R. A.; Rojas, O. J. Reinforcing poly(ε-caprolactone) nanofibers with cellulose nanocrystals. *ACS Appl. Mater. Interfaces* **2009**, *1*, 1996−2004.

(5) Sinha-Ray, S.; Zhang, Y.; Yarin, A. L.; Davis, S.; Pourdeyhimi, B. Solution blowing of soy protein fibers. *Biomacromolecules* **2011**, *12*, 2357.

(6) Khansari, S.; Sinha-Ray, S.; Yarin, A. L.; Pourdeyhimi, B. Stress-strain dependence for soy-protein nanofiber mats. *J. Appl. Phys.* **2012**, *111*, 044906.

(7) Karki, B.; Maurer, D.; Kim, T. H.; Jung, S. Comparison and optimization of enzymatic saccharification of soybean fibers recovered from aqueous extractions. *Bioresour. Technol.* **2011**, *102*, 1228.

(8) Alemdar, A.; Sain, M. Isolation and characterization of nanofibers from agricultural residues − Wheat straw and soy hulls. *Bioresour. Technol.* **2008**, *99*, 1664.

(9) Liu, K. S. *Soybeans: chemistry, technology, and utilization*; Chapman & Hall: New York, 1997.

(10) Chabba, S.; Matthews, G. F.; Netravali, A. N. 'Green' composites using cross-linked soy flour and flax yarns. *J. Green Chem.* **2005**, *7*, 576.

(11) Gennadios, A.; Brandenburg, A. H.; Weller, C. L.; Testin, R. F. Effect of pH on properties of wheat gluten and soy protein isolate films. *J. Agric. Food Chem.* **1993**, *41*, 1835.

(12) Friess, W. Collagen-biomaterial for drug delivery. *Eur. J. Pharm. Biopharm.* **1998**, *45*, 113.

(13) Wong, S. S. *Chemistry of protein conjugation and cross-linking*; CRD Press: Boca Raton, FL, 1991.

(14) Huang-Lee, L. L. H.; Cheung, D. T.; Nimni, M. E. Biomedical changes and cytotoxicity associated with the degradation of polymeric glutaraldehyde derived crosslinks. *J. Biomed. Mater. Res.* **1990**, *24*, 1185.

(15) Van Luyn, M. J. A.; Van Wachem, P. B.; Olde Damink, L. H. H.; Dijkstra, P. J.; Feijen, J.; Nieuwenhuis, P. Secondary cytotoxicity of cross-linked dermal sheep collagens during repeated exposure to human fibroblast. *J. Biomater.* **1992**, *13*, 1017.
(16) Fraonkel-Conrat, H.; Olcoh, H. S. The reaction of formaldehyde with proteins. V. cross-linking between amino and primary amide or guanidyl groups. *J. Am. Chem. Sci.* **1948**, *70*, 2673.
(17) Murata-Kamiya, N.; Kamiya, H.; Kaji, H.; Kasai, H. Mutational specificity of glyoxal, a product of DNA oxidation, in the lacI gene of wild-type *Escherichia coli* W3110. *Mutat. Res.* **1997**, *377*, 255.
(18) Vaz, C. M.; Graaf, L. A.; Reis, R. L.; Cunha, A. M. In vitro degradation behaviour of biodegradable soy plastics: Effects of crosslinking with glyoxal and thermal treatment. *Polym. Degrad. Stab.* **2003**, *81*, 65.
(19) Quero, F.; Nogi, M; Lee, K.-Y.; Poel, G. V.; Bismarck, A.; Mantalaris, A.; Yano, H.; Eichhorn, S. J. Cross-linked bacterial cellulose networks using glyoxalization. *ACS Appl. Mater. Interfaces* **2011**, *3*, 490.
(20) Katz, A. K.; Glusker, J. P.; Beebe, S. A.; Bock, C. W. Calcium ion coordination: A comparison with that of beryllium, magnesium, and zinc. *J. Am. Chem. Soc.* **1996**, *118*, 5752.
(21) Berg, J. M.; Shi, Y. The galvanization of biology: A growing appreciation for the roles of zinc. *Sci. Mag.* **1996**, *271* (5252), 1081.
(22) Zhang, J.; Mungara, P.; Jane, J. Mechanical and thermal properties of extruded soy protein sheets. *Polymer* **2001**, *42*, 2569.
(23) Fedorova, N.; Verenich, S.; Pourdeyhimi, B. Strength optimization of thermally bonded spunbonded nonwovens. *J. Eng. Fibers Fabr.* **2007**, *2*, 38.
(24) Bhat, G. S.; Jangala, P. K.; Spruiell, J. E. Thermal bonding of polypropylene nonwovens: Effect of bonding variables on the structure and properties of the fabrics. *J. Appl. Polym. Sci.* **2004**, *92*, 3593.
(25) Bhat, G. S.; Malkan, S. R. Extruded continuous filament nonwovens: Advances in scientific aspects. *J. Appl. Polym. Sci.* **2002**, *83*, 572.
(26) Michielsen, S.; Pourdeyhimi, B.; Desai, P. Review of thermally point-bonded nonwovens: Materials, processes, and properties. *J. Appl. Polym. Sci.* **2006**, *99*, 2489.
(27) Wang, X.; Michielsen, S. Morphology gradients in thermally point-bonded poly(ethylene terephthalate) nonwovens. *Text. Res. J* **2002**, *72*, 394.
(28) Otaigbe, J. U.; Adams, D. O. Bioabsorbable soy protein plastic composites: Effect of polyphosphate fillers on water absorption and mechanical properties. *J. Environ. Polym. Degrad.* **1997**, *5*, 199.
(29) Gennadios, A.; Ghorpade, V. M.; Weller, C. L.; Hanna, M. A. Heat curing of soy protein films. *Am. Soc. Agric. Eng.* **1996**, *39*, 575.
(30) Gassan, J.; Bledzki, A. K. Effect of cyclic moisture absorption desorption on the mechanical properties of silanized jute-epoxy composites. *Polym. Compos.* **1999**, *20*, 604.
(31) Pchat-Bohatier, C.; Sanchez, J.; Gontard, N. Influence of relative humidity on carbon dioxide sorption in wheat gluten films. *J. Food Eng.* **2006**, *77*, 983.
(32) Gennadios, A.; Park, H. J.; Weller, C. L. Relative humidity and temperature effects on tensile strength of edible protein and cellulose ether films. *Am. Soc. Agric. Eng.* **1993**, *36*, 1867.
(33) Cho, S. Y.; Rhee, C. Sorption characteristics of soy protein films and their relation to mechanical properties. *Lebensm. Wiss. u. Technol.* **2002**, *35*, 151.
(34) Quiocho, F. A.; Richards, F. M. The enzymic behavior of carboxypeptidase-A in the solid state. *Biochemistry* **1966**, *5*, 4062.
(35) Bedino, J. H. *Embalming chemistry: Glutaraldehyde versus formaldehyde*; Official publication of research and education department; The Champion Co: Springfield, OH, 2003; No. 649, 2614.
(36) Nayudamma, Y.; Joseph, K. T.; Bose, S. M. Studies on the interaction of collagen with dialdehyde starch. *Am. Leather Chem. Assoc. J.* **1961**, *5*, 548.
(37) *PRO-FAM 955 Isolated Soy Protein 066-955 Data Sheet*, ADM Specialty Products-Oilseeds.
(38) Consden, R.; Gordon, A. H.; Martin, A. P. The identification of amino-acid derived from cystine in chemically modified wool. *Biochem. J.* **1946**, *40*, 580.
(39) Wall, J. S. Disulfide bonds: Determination, location, and influence on molecular properties of proteins. *J. Agric. Food Chem.* **1971**, *19*, 619.
(40) de Carvalho, R. A.; Grosso, C. R. F. Properties of chemically modified gelatin films. *Braz. J. Chem. Eng* **2006**, *23*, 45.
(41) Rhim, J. W.; Gennadios, A.; Handa, A.; Weller, C. L.; Hanna, M. A. Solubility, tensile, and color properties of modified soy protein isolate films. *J. Agric. Food Chem.* **2000**, *48*, 4937.
(42) Vaz, C. M.; Doeveren, P.; Yilmaz, G.; Graaf, L. A.; Reis, R. L.; Cunha, A. Processing and characterization of biodegradable soy plastics: Effects of crosslinking with glyoxal and thermal treatment. *J. App. Polym. Sci.* **2005**, *97*, 604.
(43) Mark, J. E. *Polymer Data Handbook*; Oxford University Press, Inc.: New York, 1999.
(44) Yamashita, S. Heat-induced antigen retrieval: Mechanisms and application to histochemistry. *Prog. Histochem. Cytochem.* **2007**, *41*, 141.
(45) Shiurba, R. A.; Spooner, E. T.; Ishiguro, K.; Takahashi, M.; Yoshida, R.; Wheelock, T. R.; Imahori, K.; Cataldo, A. M.; Nixon, R. A. Immunocytochemistry of formalin-fixed human brain tissues: Microwave irradiation of free-floating sections. *Brain Res. Protoc.* **1998**, *2*, 109.
(46) Qin, Y.; Zhu, C.; Chen, J.; Liang, D.; Wo, G. Absorption and release of zinc and copper ions by chitosan fibers. *J. Appl. Polym. Sci.* **2007**, *105*, 527.